1-18-2021

# Male Fetal Sex Affects Uteroplacental Angiogenesis in Growth Restriction Mouse Model

Jessica F. Hebert
*Portland State University*

Jess A. Millar
*Portland State University*

Rahul Raghavan
*Portland State University*, rahul.raghavan@pdx.edu

Amie L. Romney
*Portland State University, University of California, Davis*, arom2@pdx.edu

Jason Podrabsky
*Portland State University*, podrabsj@pdx.edu

See next page for additional authors



## Citation Details

Hebert, Jessica F.; Millar, Jess A.; Raghavan, Rahul; Romney, Amie L.; Podrabsky, Jason; Rennie, Monique Y.; Felker, Allison; O'Tierney-Ginn, Perrie; Morita, Mayu; DuPriest, Elizabeth A.; and Morgan, Terry K., "Male Fetal Sex Affects Uteroplacental Angiogenesis in Growth Restriction Mouse Model" (2021). *Biology Faculty Publications and Presentations*. 337.
https://pdxscholar.library.pdx.edu/bio_fac/337

# Male Fetal Sex Affects Uteroplacental Angiogenesis in Growth Restriction Mouse Model

Jessica F. Hebert, Ph.D.[1,2,3], Jess A. Millar, M.S.[3], Rahul Raghavan, Ph.D.[3], Amie Romney, Ph.D[3], Jason E. Podrabsky, Ph.D.[3], Monique Y. Rennie, Ph.D.[2], Allison Felker, Ph.D.[4], Perrie O'Tierney-Ginn, Ph.D.[5], Mayu Morita, B.S. [1,2], Elizabeth A. DuPriest, Ph.D.[2,6], Terry K. Morgan, M.D., Ph.D.[1,2]

[1]Department of Pathology and the [2]Center for Developmental Health, Oregon Health & Science University, Portland, OR; [3]Department of Biology, Portland State University, Portland, OR; [4]Department of Pathology and Molecular Medicine, McMaster University, Hamilton, Ontario, Canada; [5]Mother Infant Research Institute, Tufts Medical Center, Boston, MA; [6]Division of Natural Sciences and Health, Warner Pacific University, Portland, OR.

Running Title: Fetal sex affects uteroplacental angiogenesis

Summary Sentence: Male fetal sex affects maternal uterine spiral artery angiogenesis and placental efficiency leading to intrauterine growth restriction.

Keywords: placenta, placental transport, angiogenesis, intrauterine growth restriction

Grant support: This study was funded by the *National Institute of Child Health and Human Development* (1R21HD068896-01A1), the *Office of Women's Health Research*: Oregon K12 BIRCWH (HD043488-08), the *Society of Reproductive Investigation*, and the *Oregon Medical Research Foundation*.

Conference Presentation: Society of Reproductive Investigation, March 7-11, 2019, Paris, France.

Correspondence: Terry K Morgan, MD, PhD
Department of Pathology
Oregon Health & Science University
3181 SW Sam Jackson Park Rd
Portland, OR 97239
Telephone: 503-494-2771
email: morgante@ohsu.edu

Footnote: Several authors have changed institutions since this work was completed and entered the manuscript stage. JFH is in the Department of Anesthesiology and Perioperative Medicine at Oregon Health & Science University. JAM is in the department of Computational Medicine and Bioinformatics at the University of Michigan. AR is at the School of Veterinary Medicine at UC Davis. MYR is the Scientific Affairs and Communications Manager for MolecuLight, Inc. AF is in the Department of Pathology and Molecular Medicine at McMaster University.

## Abstract

Abnormally increased angiotensin II activity related to maternal angiotensinogen (AGT) genetic variants, or aberrant receptor activation, is associated with small-for-gestational-age (SGA) babies and abnormal uterine spiral artery remodeling in humans. Our group studies a murine AGT gene titration transgenic (TG; 3-copies of the AGT gene) model, which has a 20% increase in AGT expression mimicking a common human AGT genetic variant (A[-6]G) associated with intrauterine growth restriction (IUGR) and spiral artery pathology. We hypothesized that aberrant maternal AGT expression impacts pregnancy-induced uterine spiral artery angiogenesis in this mouse model leading to IUGR. We controlled for fetal sex and fetal genotype (e.g., only 2-copy wild-type [WT] progeny from WT and TG dams were included). Uteroplacental samples from WT and TG dams from early (days 6.5 and 8.5), mid (d12.5), and late (d16.5) gestation were studied to assess uterine natural killer cell (uNK) phenotypes, decidual metrial triangle angiogenic factors, placental growth and capillary density, placental transcriptomics, and placental nutrient transport. Spiral artery architecture was evaluated at day 16.5 by contrast-perfused three-dimensional micro-computed tomography (3D microCT). Our results suggest that uteroplacental angiogenesis is significantly reduced in TG dams at day 16.5. Males from TG dams are associated with significantly reduced uteroplacental angiogenesis

from early to late gestation compared with their female littermates and WT controls. Angiogenesis was not different between fetal sexes from WT dams. We conclude that male fetal sex compounds the pathologic impact of maternal genotype in this mouse model of growth restriction.

## Introduction

Poor fetal growth is a common and potentially life-threatening complication of pregnancy [1]. Limited fetal growth may manifest as intrauterine growth restriction (IUGR), a multifactorial disorder characterized by fetal weight below the 10th percentile for gestational age relative to the population [2]. Adverse health outcomes of poor fetal growth include increased perinatal morbidity and mortality with an increased risk of adult-onset diabetes and cardiovascular disease [3-7]. Males seem to be more susceptible to the underlying pathophysiology [8] and long-term health consequences of developmental programming [4-7].

Small babies come from small placentas with gross and histologic features of maternal vascular malperfusion (placental insufficiency), including placental infarctions and accelerated villous maturation [9-14]. This may be related to insufficient delivery of nutrients (e.g., pathologic changes in the uteroplacental arterial network) and/or increased fetoplacental demand (e.g. twin gestations) [14–16]. The reason why IUGR males do more poorly than females is unknown, but it may be related to relatively increased metabolic demands [17]. In addition, male fetal sex has been associated with impaired angiogenesis in murine and porcine models of IUGR [18, 19].

Maternal uterine angiogenesis and pregnancy-induced remodeling are essential for normal pregnancy outcomes in mice and humans [9, 20, 21]. In humans, the uterine arteries (arcuate, radial, spiral) grow, coil, and dilate in a process related to a combination of angiogenic growth factors [e.g., placental growth factor (PLGF) and vascular endothelial growth factor (VEGF)] and increased blood flow into the intervillous space [22-25]. In mice, the uterine spiral arteries

grow *de novo* during early-to-mid pregnancy, highlighting the importance of this pregnancy-induced process [26].

The uterine vascular network and placental bed (a.k.a. decidua basalis in women and "metrial triangle" in mice) are very similar in mice and women [22, 26-29], but there are large differences in how the uterine and fetoplacental vascular networks interdigitate. The mouse placenta does not have an intervillous space. Instead, it is composed of a labyrinth of interdigitating capillary-like spaces lined by placental trophoblasts encasing fetoplacental capillaries [26]. The decidua in mice and women is composed of uterine natural killer cells (uNK) that are thought to play a vital role in regulating spiral artery angiogenesis. Angiogenic factors like VEGF and PLGF are released by uNK cells to stimulate angiogenesis in the decidua/metrial triangle [28, 29]. Moreover, vascular growth in both the uterus and placenta seem to rely on similar angiogenic/anti-angiogenic pathways involved in vasculogenesis (initial development of vessels) and angiogenesis (additional growth of new vessels by branching from existing vessels) to grow capillary-like networks to prune into proper arteries and capillary beds for nutrient exchange [30-32].

We hypothesize that fetal sex may impact uteroplacental angiogenesis, leading to worse clinical outcomes in males compared with females from high-risk pregnancies. To test this, we employed a murine angiotensinogen (AGT) gene titration transgenic (TG) model [33,34], which was designed to mimic a common human AGT promoter variant (A[-6]G) associated with pregnancy-induced hypertension, IUGR, and abnormal uterine spiral artery remodeling in the first trimester [35-37]. We have previously shown that this TG model has features similar to

women with preeclampsia [36] and more recently that their growth restricted progeny develop adult-onset stress-induced hypertension [34]. An advantage of this model is mice have multiple pups per litter, enabling comparison of fetal sex between siblings with wild-type (WT, 2-copy) genotypes within each litter and between litters relative to maternal genotype (WT versus TG).

## Materials and Methods

Transgenic Mouse Model: Experimental procedures were approved by the Institutional Animal Care and Use Committee of Oregon Health and Science University and were conducted in accordance with specific guidelines and standards. Angiotensinogen (AGT) 3-copy transgenic (TG) dams (B6.129P2-Agt$^{tm1Unc}$/J) were purchased from The Jackson Laboratory (Bar Harbor, Maine) and backcrossed with wild-type (WT) C57/BL6 mice from Charles River Laboratories (Wilmington, MA) for more than ten generations before experimentation, similar to our group's previous work with this model [34, 36]. Adult (11-13 weeks old) TG and WT females were bred with WT males and embryogenesis was timed from the vaginal plug (day 0.5). Fetal sex (SRY) and AGT genotype (3-copy vs. 2-copy) were determined by PCR using specific primer sets that yielded products of expected size and sequence using genomic DNA from fetal liver tissue or adult tail snips extracted by DNeasy (QIAgen; Valencia, CA) or REDExtract-n-Amp PCR Reaction Mix (Sigma-Aldrich; St. Louis, MO), respectively, as previously described [34]. Data related to maternal genotype and fetal sex were averaged per litter ($\geq$4 litters/ group/ experiment).

Tissue Samples: For each fetus, the maternal uterine metrial triangles and their corresponding placentae were isolated separately from their siblings to control for fetal sex and fetal genotype.

Only WT fetal genotypes (2-copies of AGT gene) were used for all experiments to control for the potential confounding effects of fetal 3-copy AGT expression in TG litters. Intact metrial triangles with attached placentae were evaluated at day 6.5 and 8.5 for uNK activity. Micro-dissected decidua at day 12.5 was used for angiogenic/anti-angiogenic expression analyses. Uterine vascular architecture was evaluated by contrast-perfused three-dimensional micro-computed tomography (3D microCT) imaging at day 16.5. Placental capillary density, transcriptomics, and nutrient transport studies were also evaluated at day 16.5 because of increased confidence of completed pregnancy-induced uterine angiogenesis by this time point [21]. At each gestational age from 6.5-16.5, the fetus could be readily identified and excised to provide fetal livers to determine fetal sex and fetal genotype corresponding to its placenta and maternal metrial triangle.

Three Dimensional MicroCT Measurements of Uterine Arterial Structure: Uteroplacental vasculature was perfused with x-ray contrast (Microfil HV-122, Flowtech Inc., Carver, MA) at day 16.5 as previously described [21, 38]. Briefly, perfusion was via a cannulated descending aorta with the use of a perfusion pump while monitoring the exposed uterus to enable selected fill into the uterine arteries and placental labyrinth capillary bed. 3D microCT images were acquired and reconstructed on a Quantum FX micro-CT (Caliper Life Sciences). Vascular surface renderings were visualized and measured using Amira 3D visualization software. Spiral artery number, branching, and coiling feeding each uteroplacental network were measured independently by two reviewers (MR and JH) blinded to maternal genotype and fetal sex. Averaged values for each fetal sex per each litter per maternal genotype were used for statistical analysis.

147

148 Angiogenic/Anti-angiogenic Expression Analyses: Protein extracted from micro-dissected
149 metrial triangles were analyzed using commercially available ELISAs (R&D Systems;
150 Minneapolis, MN) for soluble fms-like tyrosine kinase 1 (sFLT-1), VEGF, and PLGF according
151 to manufacturer's instructions. Each experiment was performed in triplicate and expression
152 levels were estimated by comparison with kit-provided internal standards. Values were within
153 the dynamic range of each ELISA assay and results for each fetal sex per litter per maternal
154 genotype were used for statistical analysis.

155

156 uNK Cell Phenotyping and Angiogenesis in Whole Mounts: Assessment of uterine natural killer
157 cell variable phenotype composition and metrial triangle angiogenesis in whole mount
158 experiments were performed as described by Anne Croy's group [28, 39]. Briefly,
159 immunofluorescence assays were performed at days 6.5 and 8.5 using *in situ* uteroplacental
160 whole mounts from TG and WT dams (4-6 litters/group) when uNK cell composition is
161 changing most dramatically [28]. Day 8.5 is also when vasculogenesis/angiogenesis is
162 reportedly at its peak [39]. Uteri from days 6.5 and 8.5 were bisected along the midsagittal line
163 of the mesometrial-antimesometrial axis. They were then stained with FITC-conjugated
164 *Dolichos biflorus* agglutinin (DBA) lectin (Vector Laboratories; Burlingame, CA) and PE-
165 conjugated antibody against lectin-like receptor Ly49C/I (BD Biosciences; Franklin Lakes, NJ).
166 PE-conjugated anti-CD31 (also known as platelet endothelial cell adhesion molecule (PECAM-
167 1); BD Biosciences) immunostaining highlighted endothelial cells in the metrial triangle to
168 quantify early angiogenic "blebbing" and pruning "branching metric" described by the Croy
169 group [39]. Wild-type values were compared with those reported by the Croy group [28] for

quality control and only the means per fetal sex per maternal genotype per litter were reported for scientific rigor.

Placental Metrics: Placentas corresponding to each 2-copy fetus from WT and TG litters were weighed, measured, and paraffin-embedded for stereological assessment of CD31 immunostained histologic sections to calculate fetoplacental labyrinth capillary number and density [40, 41]. Briefly, placentas were cut from a random starting point in thick systematic random sections perpendicular to the chorionic plate. The approximately four thick sections obtained per placenta were mounted into a single block (as described in [40]). Sections 5 μm thick were immunostained for CD31 to highlight endothelial cells outlining fetoplacental capillaries. One histologic section per placental block was evaluated. The placental labyrinth within each section was outlined using Stereo Investigator software (MBF Bioscience; Williston, VT). The number of capillaries within 100% of each placenta's labyrinth cross-sectional area was calculated using the point counting method [40, 41] and compared between four litters per maternal genotype.

Placental Transcriptomics: cDNA libraries were prepared from day 16.5 placentas from male and female 2-copy pups from TG and WT dams using the TruSeq RNA Sample Preparation Kit (Illumina; San Diego, CA) according to manufacturer's instructions. Purified libraries were quantified on a Bioanalyzer 2100 (Agilent; Santa Clara, CA) using a DNA 1000 chip and sequenced using Illumina HiSeq™ 2000. Reads were cleaned by removing adapters and were filtered by quality (>Q20) and length (>50 bp) using Trimmomatic v0.30 [42]. CLC-workbench (version 9.0; CLCbio) was used to map reads to *M. musculus* Genome Reference

Consortium Mouse Build 38 (GCA_000001635.6). Transcript abundance and differential gene expression on groups clustered based on PCR analysis were tested for using Empirical analysis of DGE in CLC-workbench, controlling false discovery rate at 0.05. Genes that were determined as significantly differentially expressed between/among groups were assigned gene ontology (GO) terms using Database for Annotation, Visualization, and Integrated Discovery (DAVID) [43]. GO terms were clustered using REVIGO (medium stringency) [44]. Transcript abundance was reported as RPM averages per fetal sex per maternal genotype per litter (samples from 4 litters/genotype for this –omics pilot study).

qRT-PCR Validation of RNASeq: RNA from each day 16.5 placental sample was converted to cDNA using SuperScript III First-Strand Synthesis System and amplified using TaqMan probes (Life Technologies; Carlsbad, CA) to measure expression of FLT-1, VEGF, and several genes from key gene ontologies identified by RNASeq relative to *Gapdh* baseline expression: fatty acid-binding protein 1 and 4 (*Fabp1, Fabp4),* peroxisomal acyl-coenzyme A oxidase 2 (*Acox2*), cytochrome c oxidase subunit I and II (*Cox1, Cox2*), c-type lectin domain family 2 member D (*Clec2d*), and killer cell lectin-like receptor subfamily B member 1 (*Klrb1b*) (Primers in **Supplemental Table 1**). Amplification was conducted using a Roche LightCycler as follows: 1 cycle at 95°C for 5 minutes, 40 cycles of 95°C for 15 seconds, and 65°C for 60 seconds (with acquisition at 65°C). Cycle point crossings were compared with a standard curve for each marker to quantify the relative starting amount of mRNA expressed in each sample.

Placental Nutrient Transport Assays: Placental transport of radiolabeled fatty acids and amino acids were measured *in vivo* in four TG and four WT litters at day 16.5 using previously

described methods [45-47]. Briefly, $^{3}$H-radiolabeled arachidonic acid (AA) (2µCi/kg complexed 1:1 with fatty acid-free albumin) (lipid transport) or $^{14}$C-methylaminoisobutyric acid (MeAIB) (50 µCi/kg) (amino acid transport) were administered in a 100µl PBS bolus injection via maternal jugular catheterization and samples of maternal blood were collected over 4 minutes from tail vein. After 4 minutes, placentas and fetuses were collected and weighed. Samples were solubilized with Biosol (PerkinElmer; Waltham, MA) to determine radioactivity in each fraction relative to weight. Maternal to fetal unidirectional clearance (K) for each tracer was calculated by dividing fetal counts (N) by the area under the maternal isotope concentration curve (AUC) from time 0 to sacrifice (dpm*min*µl$^{-1}$) multiplied by placental wet weight in grams (W): K=N/[AUC*W]. Experiments were performed in triplicate and reported as the means per 2-copy fetal genotype (pWT, pTG) per fetal sex per maternal genotype.

Statistical Analysis: Fetal sex and maternal genotype were the primary variables for analysis. Within each litter, average (mean) values were calculated for each sex. At least four litters per maternal genotype were used in statistical analyses. Data were analyzed by two-way ANOVA with Tukey's multiple comparisons post-hoc correction when indicated. Results were presented as means ± SEM with significance set as $p<0.05$.

## Results

*Intrauterine Growth Restriction Mouse Model*

Males from TG dams were smaller than males from WT dams both at day 16.5 (0.48 +/- 0.03g vs. 0.55 +/- 0.02g [$p$=0.05]) and at birth (1.29 +/- 0.02g vs. 1.46 +/- 0.04g [$p$=0.02]). Females

from TG dams were smaller at birth (1.23 +/- 0.01g vs. 1.37 +/- 0.02g [$p<0.001$]), but not at day 16.5 (0.48 +/- 0.04g vs. 0.52 +/- 0.02g [NS], respectively).

*Male Fetal Sex is Associated with Reduced Spiral Artery Angiogenesis in TG Dams*

Pregnancy-induced uterine spiral artery angiogenesis measured by 3D microCT imaging was significantly reduced in males from TG dams compared with their female siblings and WT controls (**Figure 1**). The number of spiral arteries per placenta was halved in male TG fetuses, but unchanged in females, and reduced coiling was also present in male, not female, TG placentas. There was no difference between males and females within WT litters, suggesting that maternal genetic risk was necessary to detect this fetal sex difference.

*Angiogenic/Anti-Angiogenic Levels in Maternal Decidua (Metrial Triangles) at Mid-Gestation*

Although peak metrial triangle angiogenesis occurs at day 8.5 in the mouse [40], micro-dissection of the fetal placenta away from the maternal decidua was not reproducible or reliable until day 12.5 in our hands (confirmed by cytokeratin immunostained histologic analysis of micro-dissected tissues—data not shown). At day 12.5, the metrial triangles associated with male pups from TG dams showed significantly less PLGF ($p<0.05$) and more sFLT-1 ($p<0.01$) with a significant shift in the sFLT-1 to PLGF ratio compared with males from WT dams ($p<0.001$) (**Figure 2**). Both fetal sexes from TG dams showed an increase in the placental FLT-1/VEGF expression ratio, although this was more pronounced in pTG males.

*uNK Cell Variable Phenotype Composition and Metrial Triangle Angiogenesis*

To test whether differences in metrial angiogenesis by fetal sex and maternal genotype could be related to a shift in uNK composition, we evaluated uteroplacental whole mounts at days 6.5 and 8.5 as described previously [28]. Decidual uNK cell composition shift was measured as the ratio of DBA+ to Ly49C/I cells per unit area. Higher ratios indicate greater angiogenic signaling since DBA+ cells produce VEGF and PLGF [39]. Metrial triangles supplying male and female fetuses from WT dams both showed an increase in DBA+ uNK cells from day 6.5 to 8.5 (**Figure 3A, B**), similar to values previously reported by the Croy laboratory [26]. Males from TG dams did not appear to have this similar change in uNK cell phenotype by day 8.5. Females from TG dams had a similar pattern to WT, although there was a greater shift in uNK composition in pTG females.

To test for differences in endothelial "blebbing" and vascular pruning [32, 39] in the metrial triangle by fetal sex and maternal genotype, we stained whole mounts for the endothelial marker CD31 and measured them as described by the Croy laboratory [28, 39]. We observed less vascular blebbing in all metrial triangles of TG dams compared with WT controls independent of fetal sex at days 6.5 and 8.5 (**Figure 3C**). Vascular pruning from day 6.5 to 8.5 led to fewer branches/area in all metrial triangles from both sexes and both maternal genotypes (**Figure 3D**). However, males from TG dams showed more pruning than their female siblings. Therefore, although both fetal sexes from TG dams had reduced angiogenic blebbing, pTG females did not prune as vigorously as their pTG male siblings. Examples of CD31 staining and DBA+/Ly49+ staining in a whole mount section can be found in **Figure 3E and 3F**, respectively.

*Placental Metrics*

Placental weights were not statistically different between pTG and pWT groups at day 16.5, but pTG males had a significantly lower fetal:placental weight ratio (index of placental efficiency) compared with controls ($p<0.05$) and their female siblings **(Figure 4A**). Placental stereometric analysis of CD31 immunostained sections **(Figure 4B)** revealed fewer capillaries per placental labyrinth cross-sectional area in pTG males compared with their pTG female siblings and WT controls (**Figure 4C**).

*Placental Transcriptomic Analysis and Placental Nutrient Transport*

To investigate whether there are differences in placental expression at day 16.5 by fetal sex and maternal genotype, we employed an exploratory placental transcriptomic approach. This time point was chosen because of reproducible micro-dissection of placental labyrinths away from maternal metrial triangles. Males from TG dams had significantly higher abundances of gene transcripts than WT controls (**Figure 5A**). There were only minimal differences in gene expression abundance between females from TG and WT dams (**Figure 5B**). Overall, 132 genes were similar in their expression between males and females from TG dams compared with matched WT controls (**Figure 5C**).

After performing GO enrichment for gene lists that were significantly different in abundance between groups (higher or lower expression than controls), we found the similar genes in pTGs were involved in the *upregulation* of lipid transport pathways, *upregulation* of oxidation-reduction, and *downregulation* of negative regulators of the innate immune response (**Figure 5D**). Validation of candidate genes within these pathways by qRT-PCR correlated well with patterns observed in RNASeq data (overall $R^2=0.98$, $p<0.001$). Notably, expression of both

*Clec2d* and *Klrb1b* was significantly downregulated in the placentas of pTG males compared to WT males. *Klrb1b* is also known as *Cd161* and is expressed by NK cells; in particular, it is linked to regulating and reducing NK cell cytotoxicity [48]. Protein KLRB1 binds to lectin-like transcript-1 (LLT1) which downregulates NK-mediated lysis; LLT1 is encoded by *Clec2d* [49]. Pathway analysis and validation of the differentially regulated genes between pTG male and female placentas is the subject of an ongoing investigation by our group. Placental nutrient transport assays at day 16.5 showed greater transport in pTG females compared with their male siblings (**Figure 5E, F**), which may represent a placental compensatory mechanism to the TG maternal phenotype.

## Discussion

Our data suggest that fetal sex may compound maternal high-risk genotypes/phenotypes, leading to abnormal uterine spiral artery angiogenesis and the cascade of events culminating in compromised fetal growth. This is an important observation because male babies have an increased risk of perinatal morbidity/mortality; they are more susceptible to long-term developmental programming of adult-onset diseases [4, 8, 50]. Although male fetal sex vulnerability is well-described, the mechanism is poorly understood.

Poor fetal growth is a multifactorial syndrome, and our model focuses on two risk factors: maternal genotype and fetal male sex. The maternal genetic high-risk mouse model mimics the 20% higher plasma AGT levels observed in humans with the A-6 AGT promoter variant [33, 35, 51, 52]. This genetic variant is a common allele present in approximately 14% of Caucasians and imparts a significantly increased risk of IUGR associated with spiral artery pathology compared

with the G-6 allele [37, 51]. In this study, we controlled for the fetal genotype by restricting analysis to 2-copy (WT) mice from TG dams to isolate the effects of fetal sex and maternal genotype in this model. Future studies will explore the impact of fetal genotype on outcomes.

We suspect male fetal sex may contribute to poor fetal growth because it appears to impact uNK composition in the uterine lining (decidua; metrial triangle) and uteroplacental angiogenesis. uNK cells are abundant in both murine and human decidua during pregnancy and are characterized as Ly49, DBA+/-, in the mouse [53]. DBA+ cells peak around days 8.5-10.5 and release pro-angiogenic factors like VEGF and PLGF [54]. Although we did not see a difference in placental invasion in the metrial triangles studied at days 12.5 and 16.5 in the model (data not shown), we cannot exclude differences in pTG male placental cell interactions with maternal uNK cells compared with controls. However, we think direct cell-to-cell interaction may not be necessary because spiral artery angiogenesis is complete by mid-gestation in mice before the placenta invades into the metrial triangle [55]. In turn, we and others are exploring the possibility that placental exosome paracrine/endocrine signaling may play a role in this process [56].

Our exploratory placental transcriptomic study suggested that maternal genotype and fetal sex may impact placental nutrient transport. We hypothesized that pTG male placentas would be less efficient and transport *fewer nutrients* to the male fetus compared with their female littermates and controls. This was reasonable because we observed a decreased fetal:placental ratio in pTG males, but not females. We were surprised to learn that pTG placentas upregulate nutrient transport genes by day 16.5 and pTG females show significantly increased amino acid transport compared with their siblings and controls. Perhaps it is not unexpected that the placentas in TG

dams transport more nutrients late in gestation compared with WT controls, despite lower birthweight. Sheep studies have shown that maternal nutrient restriction at mid-gestation leads to compensatory increases in nutrient transport and placental size by term [57]. Therefore, we now suspect that the change in placental transport observed in our study near term (day 16.5) may be compensating for relative placental insufficiency earlier in gestation and that this *compensation may be more effective in pTG females compared with their male siblings.* Another recent transcriptomics study using human placentas from first-term pregnancies indicate that males may impact extravillous trophoblast (EVT) function related to uteroplacental interface micro-environment, thus inhibiting spiral artery invasion and remodeling in human pregnancies [58]. Comparing placental expression profiles and nutrient transport earlier in gestation (e.g., days 8.5, 10.5, 12.5) will be needed to explore this hypothesis.

In summary, we tested for fetal sex effects on uteroplacental angiogenesis at early (d6.5, d8.5), mid (d12.5), and late (d16.5) gestation in a mouse model of fetal growth restriction. Males from TG dams showed significant differences compared with their female siblings and WT controls at each stage of uterine spiral artery angiogenesis from days 6.5 to 16.5. We observed fewer DBA+ uNK cells at day 6.5 and 8.5 with lower levels of pro-angiogenic factors (VEGF, PLGF) and greater anti-angiogenic sFLT-1 in the metrial triangles of pTG males. The consequence was less angiogenic blebbing, relatively greater pruning of these angiogenic networks, and significantly fewer spiral artery branches and coils by day 16.5. The impact of this altered maternal uterine vascular geometry on blood flow is only beginning to be modeled in reliable *in vivo* uteroplacental studies [19, 59]. However, one would expect that having fewer, straighter spiral arteries feeding a placenta would increase blood flow velocity, leading to greater shear stress and

turbulence [60], possibly increasing damage to the placenta and IUGR or activating endothelial cells differently than in vessels with more laminar flow. Male placentas from TG dams also expressed more FLT-1 and less VEGF mRNA compared with sex-matched WT controls, which was associated with fewer placental capillaries. This also likely contributes to poor fetal growth.

Together, our data provide a potential mechanism that may explain excessive vulnerability of males compared with females during fetal growth and development. In those exposed to maternal risk factors like maternal genotype in this model, reduced uteroplacental angiogenesis in males without compensatory increases in placental transport observed in females may result in fetal growth restriction.

**Acknowledgments:** We appreciate the generosity of Dr. Anne Croy for her contributions to our understanding of uNK cells and their important role in maternal-mediated uterine spiral artery angiogenesis in the mouse.

## References

1. Bamfo JE and Odibo AO. Diagnosis and management of fetal growth restriction. J Pregnancy. 2011; 2011:640715.

2. Peleg D, Kennedy CM, and Hunter SK. Intrauterine growth restriction: identification and management. Am Fam Physician. 1998; 58(2):453–460, 466-7.

3. Nardozza LM, Caetano AC, Zamarian AC, Mazzola JB, Silva CP, Marçal VM, et al. Fetal growth restriction: current knowledge. Arch Gynecol Obstet. 2017; 295(5):1061-77.

4. Barker DJ and Clark PM. Fetal undernutrition and disease in later life. Rev Reprod. 1997; 2(2):105–12.

5. Mondal D, Galloway TS, Bailey TC, and Mathews F. Elevated risk of stillbirth in males: systematic review and meta-analysis of more than 30 million births. BMC Med. 2014; 12:220.

6. Møller H. Change in male:female ratio among newborn infants in Denmark. Lancet. 1996; 348(9030):828–9.

7. Eriksson JG, Kajantie E, Osmond C, Thornburg K, and Barker DJ. Boys live dangerously in the womb. Am J Hum Biol. 2010; 22(3):330–5.

8. Ingemarsson I. Gender aspects of preterm birth. BJOG. 2003; 110 Suppl 20:34–38.

9. Morgan TK, Tolosa JE, Mele L, Wapner RJ, Spong CY, Sorokin Y, et al. Placental villous hypermaturation is associated with idiopathic preterm birth. J Matern Fetal Neonatal Med. 2013; 26(7):647–53.

10. Hayward CE, Lean S, Sibley CP, Jones RL, Wareing M, Greenwood SL, Dilworth MR. Placental adaptation: what can we learn from birthweight:placental weight ratio? Front Physiol. 2016; 7:28.

11. Hendrix N and Berghella V. Non-placental causes of intrauterine growth restriction. Semin Perinatol. 2008; 32(3):161–5.

12. Salafia CM, Zhang J, Charles AK, Bresnahan M, Shrout P, Sun W, Maas EM. Placental characteristics and birthweight. Paediatr Perinat Epidemiol. 2008; 22(3):229–239.

13. Gagnon, R. Placental insufficiency and its consequences. Eur J Obstet Gynecol Reprod Biol. 2003; 110 Suppl 1:S99–S107.

14. Gude NM, Roberts CT, Kalionis B, King RG. Growth and function of the normal human placenta. Thromb Res. 2004; 114(5-6):397–407.

15. Croy BA, Yamada A, DeMayo F, Adamson SL. The Guide to Investigation of Mouse Pregnancy. 2014, Academic Press.

16. Long PA and Oats JN. Preeclampsia in twin pregnancy--severity and pathogenesis. Aust N Z J Obstet Gynaecol. 1987; 27(1):1–5.

17. Clifton VL. Review: Sex and the human placenta: mediating differential strategies of fetal growth and survival. Placenta. 2010; 31 Suppl:S33–9.

18. Mangwiro YTM, Briffa JF, Gravina S, Mahizir D, Anevska K, Romano T, Moritz KM, Cuffe JSM, Wlodek ME. Maternal exercise and growth restriction in rats alters placental angiogenic factors and blood space area in a sex-specific manner. Placenta. 2018; 74:47-54.

19. Stenhouse C, Hogg CO, and Ashworth CJ. Associations between fetal size, sex and placental angiogenesis in the pig. Biol Reprod 2019; 100(1):239-252.

20. Whitley GS and Cartwright JE. Cellular and molecular regulation of spiral artery remodelling: lessons from the cardiovascular field. Placenta. 2010; 31(6):465–74.

455 21. Rennie MY, Whiteley K, Adamson SL, Sled JG. Quantification of gestational changes in the
456 uteroplacental vascular tree reveals vessel specific hemodynamic roles during pregnancy in mice.
457 Biol Reprod. 2016; 95(2): 43.
458 22. Pijnenborg R, Vercruysse L, and Hanssens M. The uterine spiral arteries in human
459 pregnancy: facts and controversies. Placenta. 2006; 27(9-10):939–58.
460 23. Luttun A, Tjwa M, and Carmeliet P. Placental growth factor (PlGF) and its receptor Flt-1
461 (VEGFR-1): novel therapeutic targets for angiogenic disorders. Ann N Y Acad Sci. 2002;
462 979:80–93.
463 24. Oh MJ, Lee JK, Lee NW, Shin JH, Yeo MK, Kim A, Kim IS, Kim HJ. Vascular endothelial
464 growth factor expression is unaltered in placentae and myometrial resistance arteries from pre-
465 eclamptic patients. Acta Obstet Gynecol Scand. 2006; 85(5):545–50.
466 25. Lash GE, Schiessl B, Kirkley M, Innes BA, Cooper A, Searle RF, Robson SC, Bulmer JN.
467 Expression of angiogenic growth factors by uterine natural killer cells during early pregnancy. J
468 Leukoc Biol. 2006; 80(3):572–80.
469 26. Adamson SL, Lu Y, Whiteley KJ, Holmyard D, Hemberger M, Pfarrer C, Cross JC.
470 Interactions between trophoblast cells and the maternal and fetal circulation in the mouse
471 placenta. Dev Biol. 2002; 250(2):358-73.
472 27. Croy BA, Burke SD, Barrette VF, Zhang J, Hatta K, Smith GN, et al. Identification of the
473 primary outcomes that result from deficient spiral arterial modification in pregnant mice.
474 Pregnancy Hypertens. 2011; 1(1):87–94.
475 28. Felker AM and Croy BA. Uterine natural killer cell partnerships in early mouse decidua
476 basalis. J Leukoc Biol. 2016; 100(4):645–655.

29. Moffett A and Loke C. Immunology of placentation in eutherian mammals. Nat Rev Immunol. 2006; 6(8):584–94.

30. Zygmunt M, Herr F, Münstedt K, Lang U, Liang OD. Angiogenesis and vasculogenesis in pregnancy. Eur J Obstet Gynecol Reprod Biol. 2003; 110 Suppl 1:S10-8.

31. Charnock-Jones DS, Kaufmann P, Mayhew TM. Aspects of human fetoplacental vasculogenesis and angiogenesis. I. Molecular regulation. Placenta. 2004; 25(2-3):103–13.

32. Ricard N and Simons M. When it is better to regress: dynamics of vascular pruning. PLoS Biol. 2015; 13(5):e1002148.

33. Kim HS, Krege JH, Kluckman KD, Hagaman JR, Hodgin JB, Best CF, et al. Genetic control of blood pressure and the angiotensinogen locus. Proc Natl Acad Sci USA. 1995; 92(7):2735–9.

34. DuPriest, EA, Hebert JF, Morita M, Marek N, Meserve EEK, Andeen N, Houseman EA, Qi Y, Alwasel S, Nyengaard J, Morgan TK. Fetal renal DNA methylation and developmental programming of stress-dependent hypertension in growth restricted male mice. Reprod Sci. 2020; 27(5):1110-1120.

35. Ward K, Hata A, Jeunemaitre X, Helin C, Nelson L, Namikawa C, et al. A molecular variant of angiotensinogen associated with preeclampsia. Nat Genet. 1993; 4(1):59–61.

36. Morgan TK, Rohrwasser A, Zhao L, Hillas E, Cheng T, Ward KJ, Lalouel JM. Hypervolemia of pregnancy is not maintained in mice chronically overexpressing angiotensinogen. Am J Obstet Gynecol. 2006; 195(6):1700–6.

37. Morgan T, Craven C, Lalouel JM, Ward K. Angiotensinogen Thr235 variant is associated with abnormal physiologic change of the uterine spiral arteries in first-trimester decidua. Am J Obstet Gynecol. 1999; 180(1 Pt 1):95-102.

499 38. Rennie MY, Rahman A, Whiteley KJ, Sled JG, Adamson SL. Site-specific increases in utero-
500 and fetoplacental arterial vascular resistance in eNOS-deficient mice due to impaired arterial
501 enlargement. Biol Reprod. 2015; 92(2):48.
502 39. Croy BA, Chen Z, Hofmann AP, Lord EM, Sedlacek AL, Gerber SA. Imaging of vascular
503 development in early mouse decidua and its association with leukocytes and trophoblasts. Biol
504 Reprod. 2012; 87(5):125.
505 40. Rennie MY, Detmar J, Whiteley K, Jurisicova A, Adamson SL, Sled JG. Expansion of the
506 fetoplacental vasculature in late gestation is strain dependent in mice. Am J Physiol Heart Circ
507 Physiol. 2012; 302(6):H1261-73.
508 41. Coan PM, Ferguson-Smith AC, and Burton GJ. Developmental dynamics of the definitive
509 mouse placenta assessed by stereology. Biol Reprod. 2004; 70(6):1806–13.
510 42. Bolger AM, Lohse M, Usadel B. Trimmomatic: a flexible trimmer for Illumina sequence
511 data. Bioinformatics. 2014; 30(15):2114–20.
512 43. Huang DW, Sherman BT, Lempicki, RA. Systematic and integrative analysis of large gene
513 lists using DAVID bioinformatics resources. Nat Protoc. 2009; 4(1):44–57.
514 44. Supek F, Bošnjak M, Škunca N, Šmuc T. REVIGO summarizes and visualizes long lists of
515 gene ontology terms. PLoS ONE 2011; 6(7):e21800.
516 45. Jones HN, Woollett LA, Barbour N, Prasad PD, Powell TL, Jansson T. High-fat diet before
517 and during pregnancy causes marked up-regulation of placental nutrient transport and fetal
518 overgrowth in C57/BL6 mice. FASEB J. 2009; 23(1):271-8.
519 46. Freeman TL, Ngo HQ, Mailliard ME. Inhibition of system A amino acid transport and
520 hepatocyte proliferation following partial hepatectomy in the rat. Hepatology. 1999; 30(2):437–
521 44.

522 47. Haggarty P, Page K, Abramovich DR, Ashton J, Brown D. Long-chain polyunsaturated fatty
523 acid transport across the perfused human placenta. Placenta. 1997; 18(8):635–642.
524 48. Pozo D, Valés-Gómez M, Mavaddat N, Williamson SC, Chisholm SE, Reyburn H. CD161
525 (Human NKR-P1A) Signaling in NK Cells Involves the Activation of Acid Sphingomyelinase. J
526 Immunol. 2006; 176:2397-2406.
527 49. Marrufo AM, Mathew SO, Chaudhary P, Malaer JD, Vishwanatha JK, Mathew PA. Blocking
528 LLT1 (CLEC2D, OCIL)-NKRP1A (CD161) interaction enhances natural killer cell-mediated
529 lysis of triple-negative breast cancer cells. Am J Cancer Res 2018; 8(6):1050-1063.
530 50. Woods LL, Ingelfinger JR, Nyengaard JR, and Rasch R. Maternal protein restriction
531 suppresses the newborn renin-angiotensin system and programs adult hypertension in rats.
532 Pediatr Res. 2001; 49(4):460–467.
533 51. Zhang XQ, Varner M, Dizon-Townson D, Song F, Ward K. A molecular variant of
534 angiotensinogen is associated with idiopathic intrauterine growth restriction. Obstet Gynecol.
535 2003; 101(2):237–42.
536 52. Morgan T, Craven C, Nelson L, Lalouel JM, Ward K. Angiotensinogen T235 expression is
537 elevated in decidual spiral arteries. J Clin Invest. 1997; 100(6):1406-15.
538 53. Yadi H, Burke S, Medeja Z, Hemberger M, Moffett A, Colucci F. Unique receptor repertoire
539 in mouse uterine NK cells. J Immunol. 2008; 181(9):6140-7.
540 54. Chen Z, Zhang J, Hatta K, Lima PD, Yadi H, Colucci F, Yamada AT, Croy BA. DBA-lectin
541 reactivity defines mouse uterine natural killer cell subsets with biased gene expression. Biol
542 Reprod. 2012; 87(4):81.
543 55. Zhang J, Chen Z, Smith GN, Croy BA. Natural killer cell-triggered vascular formation:
544 maternal care before birth? Cell Mol Immunol. 2011; 8(1):1-11.

545 56. Sheller-Miller S, Choi K, Choi C, Menon R. Cre-reporter mouse model to determine
546 exosome communication and function during pregnancy. Am J Obstet Gynecol. 2019; pii:
547 S00002-9378(19)30774-4.
548 57. Heasman L, Clarke L, Firth K, Stephenson T, Symonds ME. Influence of restricted maternal
549 nutrition in early to mid gestation on placental and fetal development at term in sheep. Pediatr
550 Res. 1998; 44(4):546-51.
551 58. Sun T, Gonzalez TL, Deng N, DiPentino R, Clark EL, Lee B, Tang J, Wang Y, Stripp BR,
552 Yao C, Tseng H-R, Karumanchi SA, Koeppel AF, Turner SD, Farber CR, Rich SS, Wang ET,
553 Williams III J, Pisarska MD. Sexually dimorphic crosstalk at the maternal-fetal interface. J Clin
554 Endocrinol Metab. 2020; 105(12):1-17.
555 59. Saghian R, James JL, Tawhai MH, Collins SL, Clark AR. Association of placental jets and
556 mega-jets with reduced villous density. J Biomech Engin. 2017; 139(5):051001.
557 60. Paszkowiak JJ, Dardik A. Arterial wall shear stress: observations from the bench to the
558 bedside. Vasc Endovascular Surg. 2003; 37(1):47-57.
559

**Figure Legends**

**Figure 1. Uterine spiral artery structure by maternal genotype and fetal sex.**

**(A)** Uteroplacental 3D microCT perfusion at day 16.5 shows uterine artery, radial arteries, and the spiral arteries that grow *de novo* during pregnancy from days 5.5 to 12.5. **(B)** There is no difference in maternal spiral artery architecture between males and females in wild-type (WT) controls. **(C)** However, males from transgenic (TG) dams show significantly fewer spiral arteries/placental unit with less spiral artery coiling/length than their female siblings or WT controls (**D)**. 2-copy progeny from 3-copy TG (pTG) dams were used for comparison with 2-copy progeny of WT dams (pWT). Data are the mean ± SEM from four litters/group. *$p$<0.05, **$p$<0.01.

**Figure 2**. **Angiogenic and anti-angiogenic factors in micro-dissected metrial triangles or placenta from mid-gestation. (A)** Example of the micro-dissected metrial triangle, placenta, and fetus at day 12.5. Metrial triangle tissue homogenates were used to measure **(B)** VEGF, **(C)** PLGF, and **(D)** sFLT-1 in WT and TG dams relative to fetal sex and 2-copy [pWT and pTG] fetal genotype. Metrial triangle anti-angiogenic sFLT-1 to pro-angiogenic VEGF **(E)** and PLGF **(F)** indices. **(G)** Relative placental FLT-1/VEGF mRNA expression indices. Data are means ± SEM from six litters/group. *$p$<0.05, **$p$<0.01, ***$p$<0.001.

**Figure 3. Uterine natural killer cell variable phenotype composition changes, metrial triangle angiogenesis and vascular pruning in early gestation.** uNK cell composition in metrial triangles expressed as the ratio of DBA+/Ly49 cells per unit area by male **(A)** and female **(B)** fetal sex controlling for fetal genotype (2-copy only) and maternal genotype (WT and TG)

revealed the expected increase in pro-angiogenic uNK cells by day 8.5 compared with day 6.5 in both sexes from WT dams. Males from TG dams failed to show this increase. However, females from TG dams had more DBA+ uNK cells than females from WT dams. **(C)** CD31 positive endothelial "blebbing," which is an indicator of early angiogenesis, was more common in the metrial triangles of WT dams, independent of fetal sex. **(D)** Vascular branching/unit area reduced as the angiogenic networks were pruned into proper arteries. Females from TG dams had significantly less overall pruning with more residual branching at day 8.5. Data are the means ± SEM of four litters/group. *$p$<0.05; **$p$<0.01; ***$p$<0.001. (E) Representative staining of blood vessels (CD31, red) in a day 6.5 female transgenic mouse at 20x magnification. (F) Representative staining of DBA+ (green) and Ly49 (red) uNK cells in a day 6.5 female transgenic mouse at 20x magnification.

**Figure 4. Placental efficiency and capillary density. (A)** Placental efficiency, which is the ratio of fetal weight to placental weight, was significantly reduced in males from TG dams compared with their female siblings and WT controls. Stereometric analysis of CD31 immunostained placental histologic sections at day 16.5 **(B)** revealed that placental capillary density was also reduced in male placentas from TG dams (**C).** Data are the means ± SEM of four litters/group. *P<0.05, **P<0.01, ***P<0.001.

**Figure 5. Placental transcriptomics and placental nutrient transport.** Volcano plots showing expression differences for **(A)** male and **(B)** female (2-copy) progeny of TG dams compared with sex-matched (2-copy) progeny of WT dams revealed significant transcript differences at day 16.5 with more upregulation and downregulation of placental genes

expressed by pTG males compared with controls. **(C)** pTG males and females shared ~132 genes that had differential transcript abundances compared with age and sex-matched pWT controls, which when classified according to ontogeny **(D)** indicated enrichment as upregulation (red) of lipid metabolism and oxidative stress pathways with downregulation (green) of the negative regulation of the innate immune response. The x-axis represents a scale of fold change (positive and negative) in transcript abundance between groups. Placental lipid transport measured by radio-labeled arachidonic acid (AA) **(E)** and amino acid transport measured by methylaminoisobutyrate (MeAIB) **(F)** showed slightly increased placental nutrient transport in pTG female progeny at day 16.5. Data are the means +/- SEM from four litters/group. *$P<0.05$

**Supplemental Table 1. Representative lipid transport regulation, innate immune response, and placental *Flt-1, Vegfa* genes tested by qRT-PCR.**

| Gene Name | Selected Related Gene Ontology Groups p<0.05 | RefSeq |
|---|---|---|
| *Fabp1* | GO:0008289 | NM_017399.4 |
| *Fabp4* | GO:0050727 | NM_024406.2 |
| *Acox2* | GO:0016042, GO:0005777, GO:0055114, GO:0006631, GO:0016054 | NM_001161667.1, NM_053115.2 |
| *Cox1* | GO:0020037, GO:0009055, GO:0055114 | NCBI Gene ID: 17708 |
| *Cox2* | GO:0020037, GO:0009055, GO:0055114 | NCBI Gene ID: 17709 |
| *Clec2d* | GO:0045824, GO:0045088, GO:0002697, GO:0002716, GO:0031342, GO:0006952, GO:0031341 | NM_053109.3 |
| *Klrb1b* | GO:0045824, GO:0031342, GO:0031341 | NM_030599.4 |
| *Flt-1* | GO:0001569, GO:0048010 | NM_010228 |
| *Vegfa* | GO:0001569, GO:0048010 | NM_01025250.3 |
| *Gapdh* | Control | NM_01289726.1 |

**<u>Supplemental Table 2.</u> Antibodies used in publication.**

| Protein Target | Name of Antibody | Manufacturer and Catalog Number | Raised in Which Species; Mono or Polyclonal | RRID |
|---|---|---|---|---|
| CD31 | Rat Anti-CD31 Monoclonal Antibody, Phycoerythrin Conjugated, Clone MEC 13.3 | BD Biosciences Cat #553373 | Rat ab; monoclonal | AB_394819 |
| Ly49C/I | Mouse Anti-Ly-49C, Ly-49I Monoclonal Antibody, Phycoerythrin Conjugated, Clone 5E6 | BD Biosciences Cat #553277 | Mouse ab; monoclonal | AB_394751 |

# Figure 1

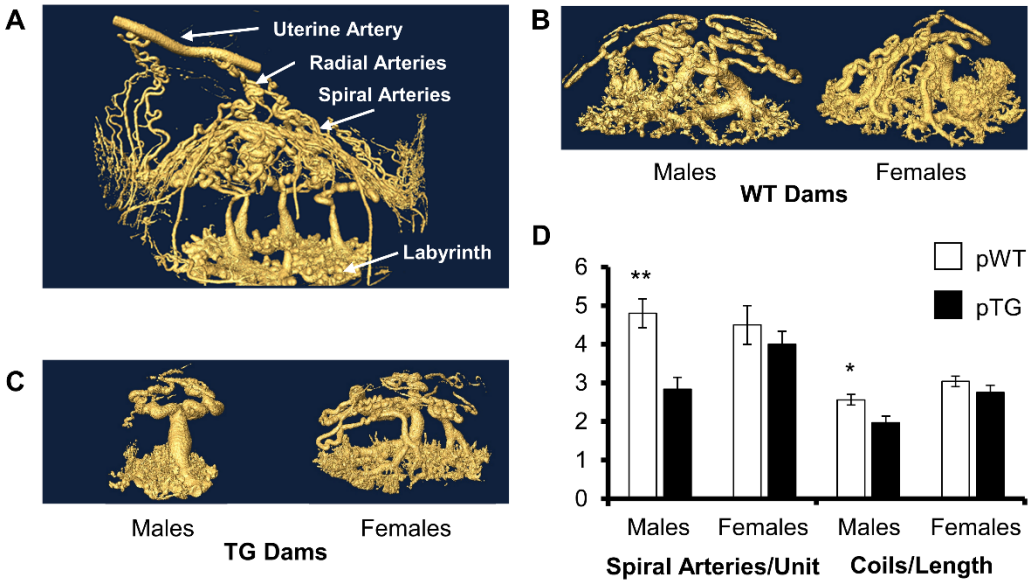
A
Uterine Artery
Radial Arteries
Spiral Arteries
Labyrinth
B
Males
Females
WT Dams
C
Males
Females
TG Dams
D
pWT
pTG
6
5
4
3
2
1
0
**
*
Males
Females
Males
Females
Spiral Arteries/Unit
Coils/Length

# Figure 2

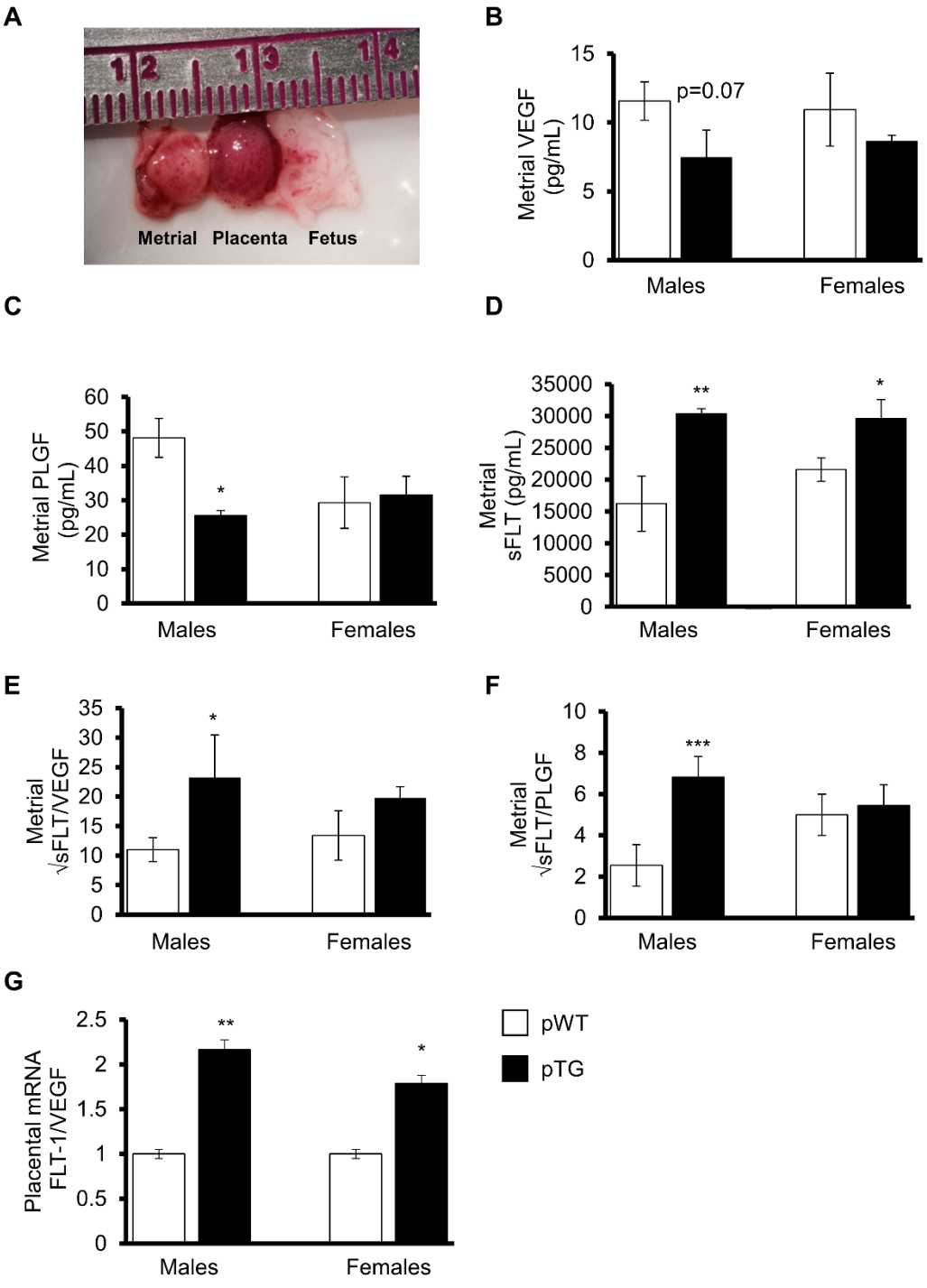
A
Metrial
Placenta
Fetus
B
Metrial VEGF (pg/mL)
p=0.07
Males
Females
C
Metrial PLGF (pg/mL)
Males
Females
D
Metrial sFLT (pg/mL)
Males
Females
E
Metrial √sFLT/VEGF
Males
Females
F
Metrial √sFLT/PLGF
Males
Females
G
Placental mRNA FLT-1/VEGF
Males
Females
pWT
pTG

# Figure 3

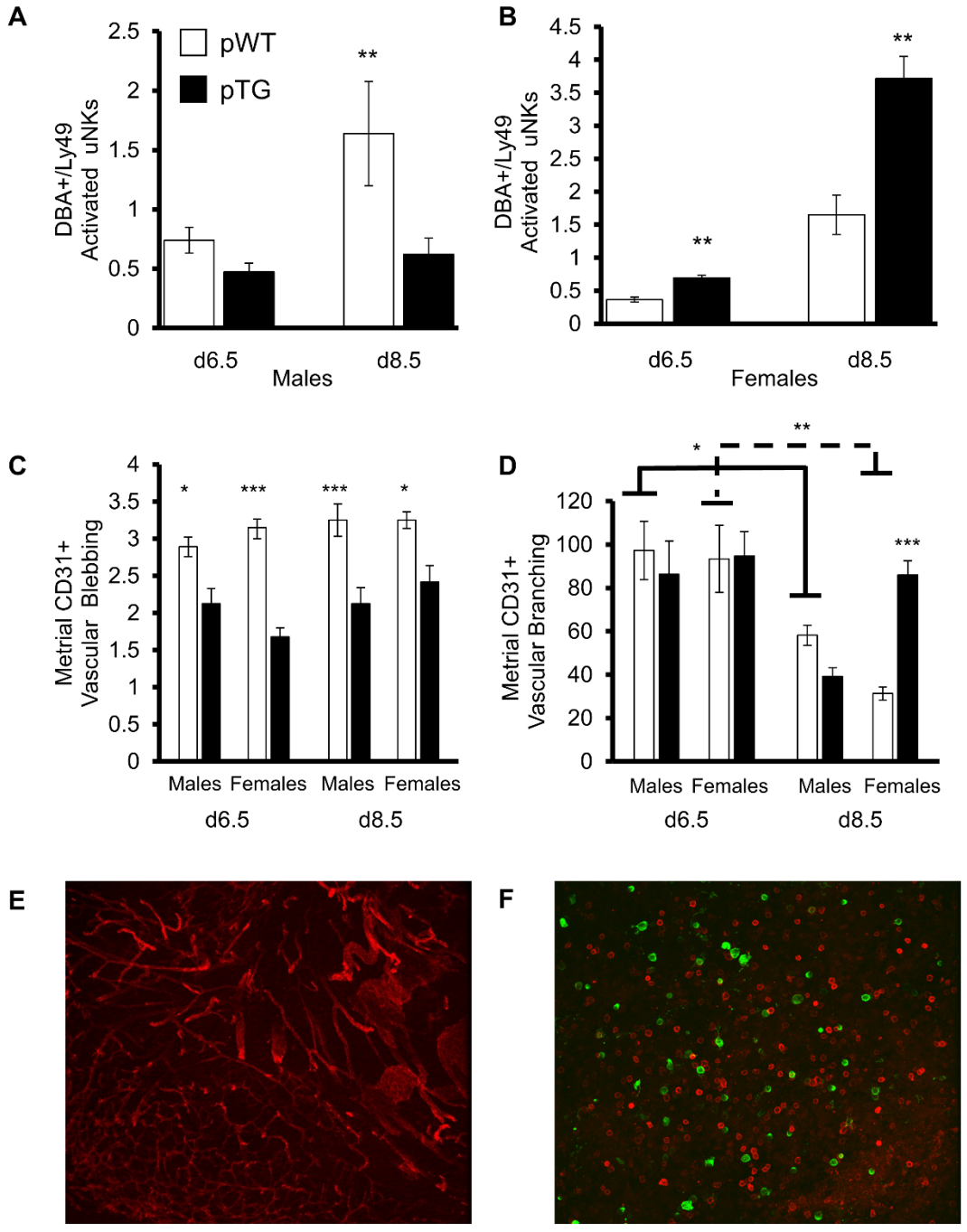
A
pWT
pTG
DBA+/Ly49 Activated uNKs
2.5
2
1.5
1
0.5
0
**
d6.5
d8.5
Males
B
DBA+/Ly49 Activated uNKs
4.5
4
3.5
3
2.5
2
1.5
1
0.5
0
**
**
d6.5
d8.5
Females
C
Metrial CD31+ Vascular Blebbing
4
3.5
3
2.5
2
1.5
1
0.5
0
*
***
***
*
Males Females Males Females
d6.5
d8.5
D
Metrial CD31+ Vascular Branching
120
100
80
60
40
20
0
*
**
***
Males Females Males Females
d6.5
d8.5
E
F

# Figure 4

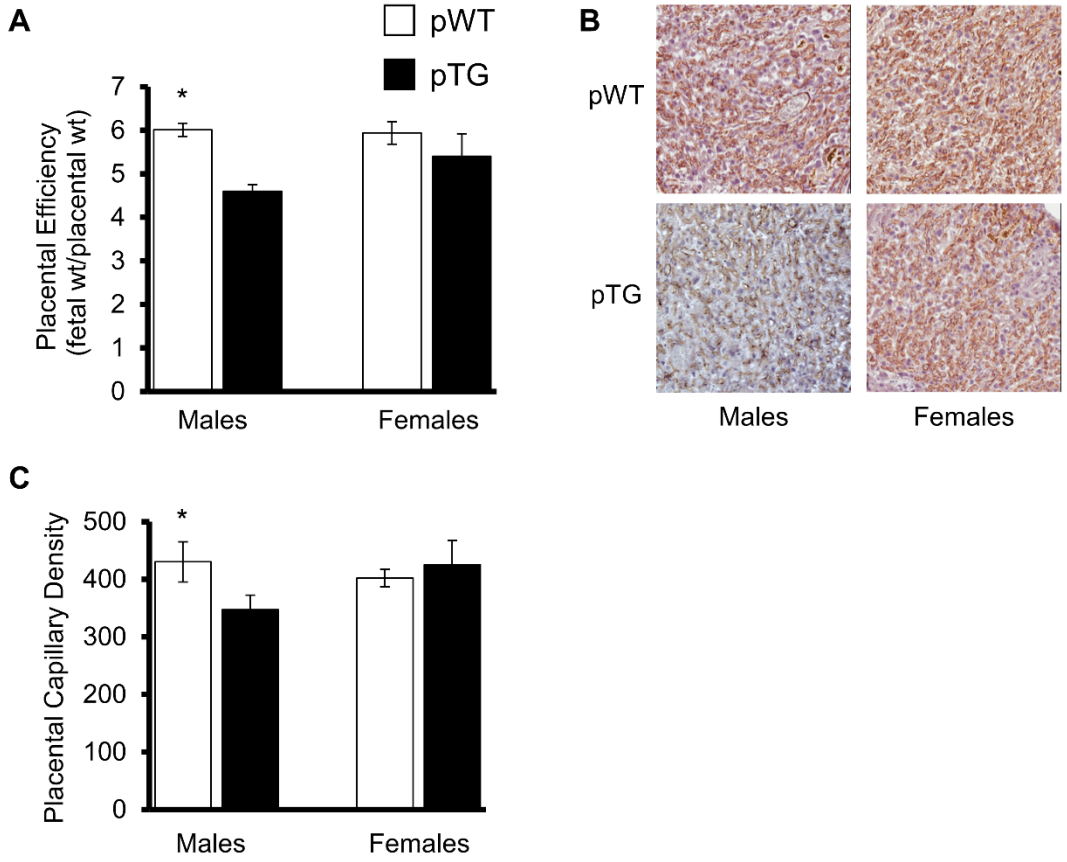
A
pWT
pTG
Placental Efficiency
(fetal wt/placental wt)
0
1
2
3
4
5
6
7
*
Males
Females
B
pWT
pTG
Males
Females
C
Placental Capillary Density
0
100
200
300
400
500
*
Males
Females

# Figure 5

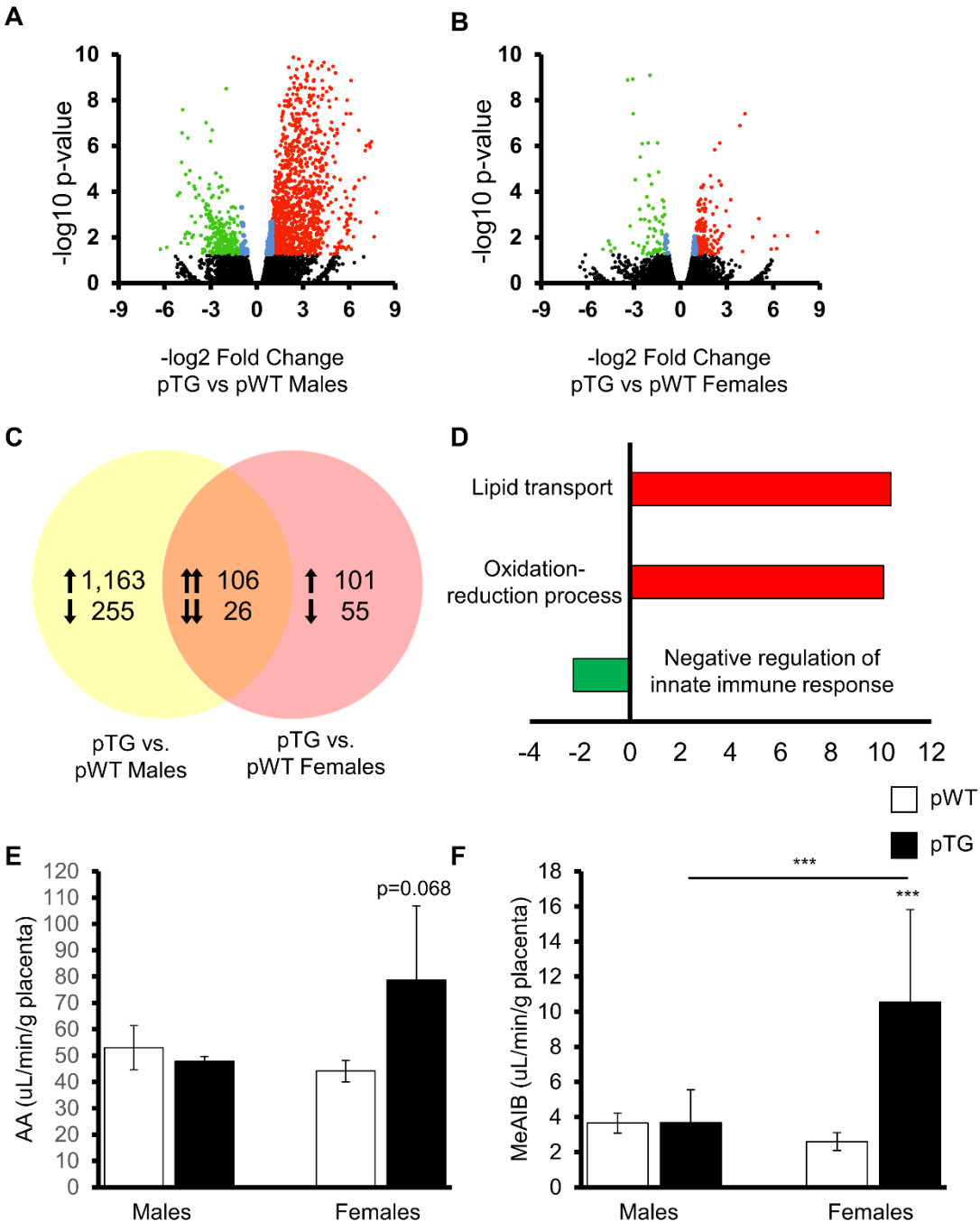
A
B
-log10 p-value
-log2 Fold Change
pTG vs pWT Males
pTG vs pWT Females
C
1,163
255
106
26
101
55
pTG vs.
pWT Males
pTG vs.
pWT Females
D
Lipid transport
Oxidation-
reduction process
Negative regulation of
innate immune response
pWT
pTG
E
AA (uL/min/g placenta)
p=0.068
Males
Females
F
MeAIB (uL/min/g placenta)
***
***
Males
Females